

## Fracture property of steel fiber reinforced concrete at early age

Chuan-Qing Fu<sup>1,2</sup>, Qin-yong Ma<sup>\*2</sup>, Xian-yu Jin<sup>3</sup>, A.A. Shah<sup>4</sup> and Ye-Tian<sup>3</sup>

<sup>1</sup>College of Civil Engineering and Architecture, Zhejiang University of Technology,  
18 Chaowang Road, Hangzhou 310034, China

<sup>2</sup>College of Civil Engineering and Architecture, Anhui University of Science and Technology,  
168 Shungong Road, Huainan 232001, China

<sup>3</sup>College of Civil Engineering and Architecture, Zhejiang University,  
866 Yuhangtang Road, Hangzhou 310058, China

<sup>4</sup>Department of Civil Engineering, Sarhad University of Science and Information Technology, Ring Road,  
Peshawar 25000, Pakistan

(Received September 6, 2011, Revised September 2, 2013, Accepted September 18, 2013)

**Abstract.** This research is focused on obtaining the fracture property of steel fiber reinforced concrete (SFRC) specimens at early ages of 1, 2, 3 and 7-day, respectively. For this purpose, three point bending tests of nine groups of SFRC beams with notch of 40mm depth and different steel fiber ratios were conducted. The experimental results of early age specimens were compared with the 28-day hardened SFRC specimens. The test results indicated that the steel fiber ratios and curing age significantly influenced the fracture properties of SFRC. A reasonable addition of steel fiber improved the fracture toughness of SFRC, while the fracture energy of SFRC developed with curing age. Moreover, a quadratic relationship between splitting strength and fracture toughness was established based on the experiment results. Additionally, a finite element (FE) method was used to investigate the fracture properties of SFRC. A comparison between the FE analysis and experiment results was also made. The numerical analysis fitted well with the test results, and further details on the failure behaviors of SFRC could be revealed by the suggested numerical simulation method.

**Keywords:** concrete; steel fiber; SFRC; early-age; fracture energy; fracture toughness; FE method

### 1. Introduction

The steel fiber-reinforced concrete (SFRC) can be considered as a composite made by concrete matrix and short steel fibers randomly distributed in the matrix. The aim of such reinforcement is to improve the mechanical behavior of the material when tensile forces are acting (Wang *et al.* 2008). Especially, when the matrix has cracked do the fibers contribute by bridging the cracks (Shah and Ribakov 2011a, Shah *et al.* 2012). Therefore, the steel fiber can limit the inner micro-crack extending and macro-crack appearing, and improve the post-cracking behavior of SFRC (Juárez *et al.* 2007). It has been reported that the fiber-reinforced concrete (FRC) containing

---

\*Corresponding author, Professor, E-mail: [qyma@aust.edu.cn](mailto:qyma@aust.edu.cn)

short fibers can also achieve a strain hardening type response when the fiber content is high enough (Li *et al.* 1998). In the last few decades, fiber reinforced cementitious materials were being increasingly employed in structural applications (Soulioti *et al.* 2009, Aggelis *et al.* 2011).

It is well known that the main role of fibers in concrete is to increase the ductility of concrete and bridge the cracks that develop in concrete. Fibers increase the strain at peak load, and provide additional energy absorption ability of RC elements and structures (Pereira *et al.* 2008, Shah and Ribakov 2011b). It was recently reported that they also considerably improve static flexural strength of concrete as well as its impact strength, tensile strength, ductility and flexural toughness (Shah 1991, Mohammadi *et al.* 2008), and also enhance the torsional moment capacities (Chalioris and Karayannis 2009). Owing to the bridging behavior of steel fiber in concrete materials, both the fracture toughness and fatigue property of SFRC are improved significantly (Uygunoqlu 2008, Shah and Ribakov 2010, Shah *et al.* 2013). The experimental results show that the bridging stress is related primarily to the interfacial bond between fiber and matrix (Zhang *et al.* 2001). With the enhancing of concrete matrix strength, the interfacial bond will be strengthened (Qian and Indubhushan 1999, Shah and Hirose 2010).

Based on the outstanding cracking resistance of SFRC in structure construction, many attempts have been made to study the fracture behavior of SFRC. A basic parameter for measuring the fracture behavior of cementitious materials is the fracture energy. Moreover, the fracture energy of conventional SFRC is independent on the specimen size and can be used to evaluate the properties of SFRC with different matrix strength (Kurihara *et al.* 2000). In previous studies, though different methods have been proposed for estimating the fracture energy experimentally, the most common way of measuring the fracture energy in concrete materials is the method proposed by RILEM TC 50-FMC (Bencardino *et al.* 2010). Carpinteri and Brighenti (2010) experimentally determined the main mechanical characteristics and fracture behavior of the pre-cracked plain concrete and fiber-reinforced concrete specimens, for different values of the water/cement ratio and different amount and type (metallic or polymeric) of reinforcing fibers, by evaluating the fracture energy. Caggiano *et al.* (2012) focused on examining the results of four-point bending tests performed on notched prisms with two different fiber content and five different combinations of long and short fibers, studied the fracture behavior of SFRC, and then, a non-linear cracked hinge model was presented. In summary, the fracture performance of steel fiber depends on fiber type (Caggiano *et al.* 2012, Michels *et al.* 2013) and orientation of fibers in matrix, fiber volume fraction (Köksal *et al.* 2002, Yazıcı *et al.* 2007), aspect ratio (length/diameter), tensile strength of fiber and matrix influence (Shah and Ribakov 2011a).

It is essential to conduct both experimental and numerical investigations on SFRC fracture behaviors. With the rapid development of computer technology and the advancement of software techniques, numerical simulation of SFRC structural response to static or dynamic loading has become feasible (Teng *et al.* 2008). It has been, however, recognized generally that the constitutive relations of SFRC plays a major role in the reliable predication of structural responses (Wang *et al.* 2010). Moreover, Constitutive models for SFRC can be classified in macro-models and micro-models according to the scale in which they are defined (Luccioni *et al.* 2012). The macro-models regard SFRC as a unique material with average properties, in which the constitutive laws are drawn from test results. Compared the macro-models to micro-models, the fiber volume fraction, aspect ratio, fiber type, distribution and orientation cannot be taken into account in the macro-models. In contrast, the main parameters of macro-models can be obtained by tensile experiment of SFRC (Olivito and Zuccarello 2010, Han *et al.* 2006).

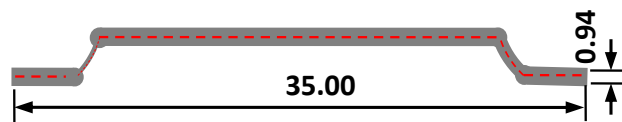
However, previous studies on fracture property of SFRC mainly focused on the test results at

the age of 28-day. No serious attention has been paid on the fracture property of SFRC at early age, especially before 7-day. But in fact, the properties of young concrete seriously affect the long term performance of mature concrete, and it is also important to the construction quality of concrete structures. In this research, to evaluate the fracture property of young SFRC, three-point bending test was conducted with simply supported notched beams. Based on the experiment results, the fracture behavior of young SFRC was analyzed, and a numerical simulation on the generation and expansion of cracks in young SFRC was carried out with ABAQUS, a FE program. The FE analysis indicates that an appropriate numerical simulation can represent the real fracture property of SFRC.

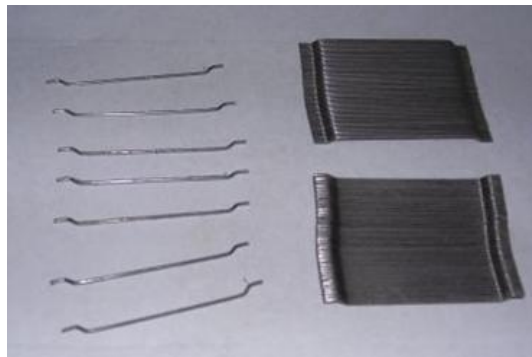
## 2. Aims, scope, and potential outcomes

This research is aimed at performing an experimental study to examine fracture property of early age SFRC, and exploring an efficient finite element method to simulate the fracture behavior of SFRC. The three-point bending test was conducted on pre-notched early SFRC beams with different curing age and fiber dosage. As an important parameter, the fracture energy was used to evaluate the fracture property of SFRC. Additionally, an effective FE method based on ABAQUS was proposed by considering the different material behavior of PC and SFRC.

The outcomes of present study will provide a comprehensive understanding on fracture properties of SFRC with different curing age and fiber dosage. On the basis of FE method, the whole fracture process and stress distribution of each calculation step can be presented. Therefore the obtained results are expected to be useful for predicting the fracture properties of different age and optimizing the fiber content fraction in concrete with different matrix strength.



(a) Shape and dimensions of the steel fibers (Dimensions: mm)



(b) Appearance of the steel fibers

Fig. 1 Steel fibers used in the study

### 3. Experiment setup

#### 3.1 Materials and mix design

The cement used in this research was Type I Portland cement with the specific surface area of  $350\text{m}^2/\text{kg}$  and the average particle diameter of  $18.27\mu\text{m}$ . The sand was natural river sand with a fineness modulus of 2.6. Crushed limestone with the maximum size of 20 mm was applied as the coarse aggregate. Herein, a kind of worldwide used steel fiber, named as Dramix, was applied. The tensile strength, elastic modulus and aspect ratio (length-to-diameter) of the hooked-end steel fiber were 1050 MPa, 210 GPa and 37.2, respectively. The shape dimensions can be seen in Fig. 1. Four kinds of concrete with the steel fibers ratio of 0%, 0.6%, 1.2% and 1.8% were named as PC, SF<sub>a</sub>, SF<sub>b</sub> and SF<sub>c</sub>, respectively. The water-to-cement ratio of all SFRCs was 0.43, and the sand ratio was 48%. The concrete mixture was made with 390 kg of cement, 863 kg of river sand, 944 kg of coarse aggregate, and 168 kg of water per  $\text{m}^3$  concrete.

#### 3.1 Sample preparation

Altogether 40 pre-notched prismatic beams (10 groups) of size,  $100\text{ mm} \times 100\text{ mm} \times 400\text{ mm}$  were cast in steel molds. Depth of the notch,  $a_0$ , was 40 mm, and the width was 3 mm (the notch tip width was 0.2 mm). The span length,  $S$ , was set as 300 mm, and the depth of the three-point bending beam,  $D$ , was 100 mm. More details can be seen in Fig. 2. All the specimens were demolded after 24 hours, and then cured under the temperature of  $(23 \pm 2)$  degree centigrade and the relative humidity of 100%.

#### 3.2 Sample preparation

Altogether 40 pre-notched prismatic beams (10 groups) of size,  $100\text{ mm} \times 100\text{ mm} \times 400\text{ mm}$  were cast in steel molds. Depth of the notch,  $a_0$ , was 40 mm, and the width was 3 mm (the notch tip width was 0.2 mm). The span length,  $S$ , was set as 300 mm, and the depth of the three-point bending beam,  $D$ , was 100 mm. More details can be seen in Fig. 2. All the specimens were demolded after 24 hours, and then cured under the temperature of  $(23 \pm 2)$  degree centigrade and the relative humidity of 100%.

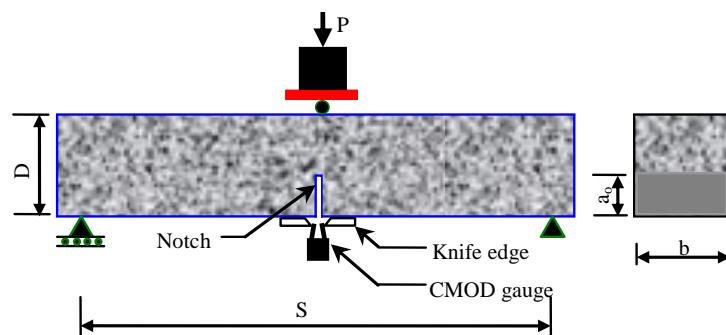


Fig. 2 Test set-up for notched beam specimen

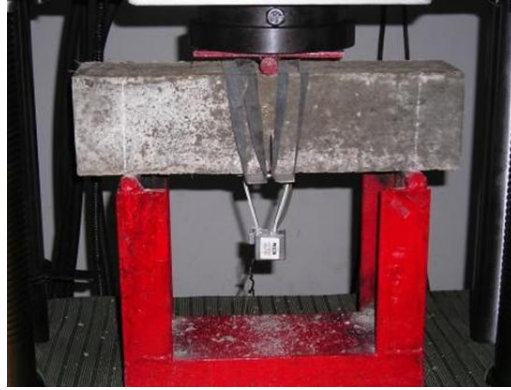


Fig. 3 Test specimen

### 3.3 Testing procedure

The fracture test apparatus used was computer controlled electro-hydraulic servo universal testing machine, WAW-1000, which is shown in Fig. 3. The crack mouth opening displacement (CMOD) was taken as the feedback.

The fracture tests on the specimens with the fiber ratio of 1.2% at 1, 2, 3, 7, and 28-day, and the specimens with different fiber ratios of 0.6% and 1.8% at the age of 7, and 28-day, were carried out. Two knife edges were attached at the bottom of the specimen on both sides of the crack mouth and a CMOD gauge was fitted to monitor and measure the CMOD during the test. The loading rate was controlled as 0.5mm/min, and the load-CMOD curves were recorded by computer system.

## 4. Test results and discussion

### 4.1 Fracture toughness

A typical load-displacement curve is shown in Fig. 4. The load-displacement curve has two load peaks, and the pre-crack energy and post-crack energy was divided by the first load peak value and its corresponding displacement value.

Test results of SFRC specimens at different ages are shown in Table 1, in which  $\rho_f$  is the fiber ratio,  $F_u$  is the ultimate load,  $F_{cra}$  is the cracking load and  $K_{IC}$  is the fracture toughness. It can be seen that the load value of SF<sub>b</sub>, including  $F_{cra}$  and  $F_u$ , has a rapid progress at the early age, especially in 3d. But the growth slows down from 7d to 28d. And the development of fracture toughness,  $K_{IC}$ , has the same trend as load value.

$K_{IC}$  of SF<sub>b</sub> is plotted against curing age in Fig. 5, in which the fitting curve was also given. We can get the relationship between  $K_{IC}$  and  $t$  as follows

$$K_{IC} = 2.235 - 10.570 / (1 + e^{\frac{t+10.876}{7.857}}) \quad (1)$$

where,  $K_{IC}$  is the fracture toughness,  $\text{MPa} \cdot \sqrt{\text{m}}$ ,  $t$  is the curing age, days.

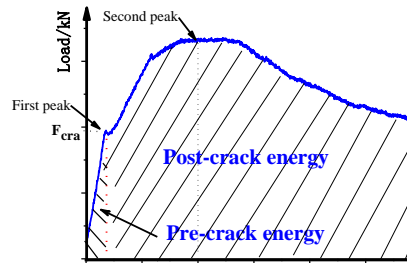


Fig. 4 A typical curve of LOAD- CMOD with SFRC beam

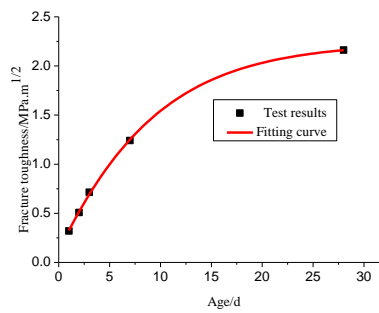


Fig. 5 Relationship between fracture toughness and curing age

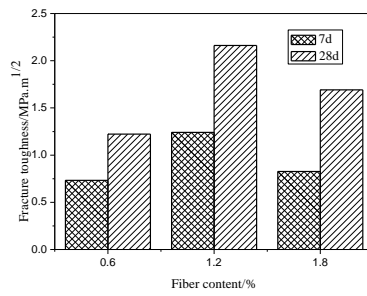


Fig. 6 Relationship between fracture toughness and curing age

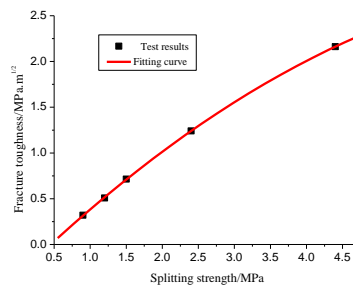


Fig. 7 Relationship between fracture and splitting strength

Table 1 Test results of load value and fracture toughness

Beam sample	$\rho_f$ (%)	$F_u$ (kN)	$F_{cra}$ (kN)	$K_{IC}$ (MPa $\cdot\sqrt{m}$ )
SF <sub>b</sub> 1	1.2	1.7	1.0	0.3196
SF <sub>b</sub> 2	1.2	2.7	1.2	0.5076
SF <sub>b</sub> 3	1.2	3.8	2.7	0.7144
SF <sub>a</sub> 7	0.6	3.9	3.3	0.7332
SF <sub>b</sub> 7	1.2	6.6	4.1	1.2408
SF <sub>c</sub> 7	1.8	4.4	3.3	0.8272
SF <sub>a</sub> 28	0.6	6.5	4.4	1.2220
SF <sub>b</sub> 28	1.2	11.5	6.2	2.1620
SF <sub>c</sub> 28	1.8	9.0	4.8	1.6920

**Notes:** Data in the table above are average value, the nomenclature of sample ID, such as SF<sub>b</sub>1, SF is the steel fiber reinforced concrete, *b* is denoted as fiber ratio and 1 is the curing age.

Table 2 Splitting strength of SF<sub>b</sub> at different curing age

Curing age (day)	1	2	3	7	28
Splitting strength(MPa)	0.9	1.2	1.5	2.4	4.4

**Notes:** The dimension of specimens used in splitting strength is 150 mm×150 mm×150 mm cube. The curing condition of the cubes was the same of the beams used in fracture toughness test.

Obviously, the curing age affected the fracture toughness significantly in the early age. In that the hydration products of cement particles filling the inner space of concrete continuously and interface between steel fiber and concrete would become dense. With the progress of cement hydration, fast in the first 3d and slow down in the after days, the bond strength will increase gradually. Hence, the effect of steel fiber can be more and more apparent.

The influence of fiber content on fracture toughness is shown in Fig. 6. Considering the above reasons and the fact that improper fiber content may lead to a bad composite. When the fiber content increases from 0.6% to 1.2%, fracture toughness increases compared to the first day by 70% and 77%, respectively. However, it should be also noticed that the fracture toughness will drop obviously when the fiber content exceeds 1.2%. The test results indicate that the fracture toughness will not increase linearly with the increase of fiber content. There exists a threshold in fiber content to improve the mechanical properties of SFRC. With the increase of fiber content within reasonable limits, the fracture toughness will increase. Once the fiber content exceeds the reasonable value, for example, 1.2% in this research, steel fiber addition will not improve the fracture toughness any more.

It can be seen in Table 1, the cracking load and ultimate load will increase 20% and 40% respectively, when the fiber content increasing from 0.6% to 1.2% at the age of 7d. However, excessive steel fiber in concrete results in weaker bonding between the interfaces, as for example the case of 1.8%. In that case the mechanical behavior was negatively influenced.

The fracture toughness is improved by increasing the tensile strength. So, there must be some relationship between fracture toughness and tensile strength. The splitting tensile test is easier than fracture toughness test. If the relationship can be established, the splitting strength will be

an indirect method to predict the fracture toughness or to verify the fracture toughness. The splitting strength of the cubes with different curing age was given in Table 2. The relationship of fracture toughness and splitting strength were presented in Fig. 7, through fitting the test results, we can get the relationship as follows:

$$K_{IC} = -0.3361 + 0.7641f_t - 0.0446f_t^2 \quad (2)$$

where,  $f_t$  is the splitting tension strength, MPa.

#### 4.2 Fracture energy

CMOD values at cracking load,  $(\text{CMOD})_{F_{\text{cra}}}$ , and ultimate load,  $(\text{CMOD})_{F_{\text{max}}}$ , are listed in Table 3, so as the fracture energy,  $G_F$ . It can be concluded from Table 3 that  $(\text{CMOD})_{F_{\text{cra}}}$  increases with the increase of curing age, but  $(\text{CMOD})_{F_{\text{max}}}$  shows the opposite trend. It is because that the strength of cement matrix increasing with the curing age, it results in the enhancement of concrete brittleness, however, improved the bond strength. If the fiber ratio is under the threshold value, the CMOD will increase.

The relationship between fracture energy and curing age was shown in Fig. 8. We can get the relationship between  $G_F$  and  $t$  as follows

$$G_F = -14802.8xe^{-t/12.96} + 15428.97 \quad (3)$$

where,  $G_F$  is the fracture energy,  $\text{N} \cdot \text{m}$ ,  $t$  is the curing age, day.

According to interface effect theory, with the increase of matrix strength, the pulling out of steel fiber from concrete matrix will consume more energy. So, the fracture energy of SFRC will increase with the increase of curing age. Compared the crack surface of plain concrete with the SFRC specimens, we can see that the crack expanded straightly; however, the crack surface of SFRC is tortuous obviously with the distribution of steel fiber. The tortuous crack propagation path significantly improved the fracture energy.

In order to understand how the steel fiber ratio affects the fracture energy, the relationships between steel fiber ratios and fracture energy are presented in Fig. 9. When the fiber content increases from 0.6% to 1.2%, the fracture energy grows 38.1% and 69.5% respectively at the age of 7d and 28d. Obviously, influenced by the two important factors of curing age and fiber content, the fracture energy was improved significantly with the growth of age and suitable increasing

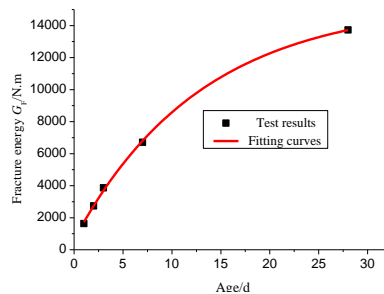


Fig. 8 Relationship between fracture energy and age

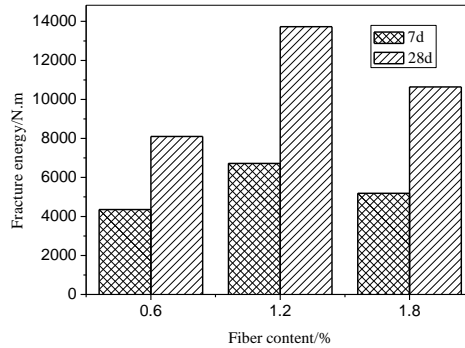


Fig. 9 Relationship between fracture energy and age

of fiber content. During the process of crack expansion, the steel fiber bridging in the main crack will be pull out and the end-hook will be straightened, which should consume much energy owing to the interfacial debonding, friction slip between fiber and matrix, and fiber distribution. The close combination of steel fiber and matrix made SFRC as an excellent composite, and the steel fiber can weaken the stress concentration in the crack tip, therefore, it limits the crack propagation and new crack generation

#### 4.3 The LOAD Vs. CMOD curves

Based on the test results, the average LOADVs. CMOD curves of SFRC at different curing ages are presented in Fig. 10. Results of experimental bending tests have shown an extended post-peak softening behavior. The shape of the descending branch depends on the geometrical and mechanical properties of the fibers and on the amount of fiber used (Zhang *et al.* 2001). All the curves presented a second peak load after the cracking load, and then a softening behavior started in the curves. The second peak load will exceed the first peak load value in the later time, and the difference in the two peak values would increase with curing time. It is worth noting that the first

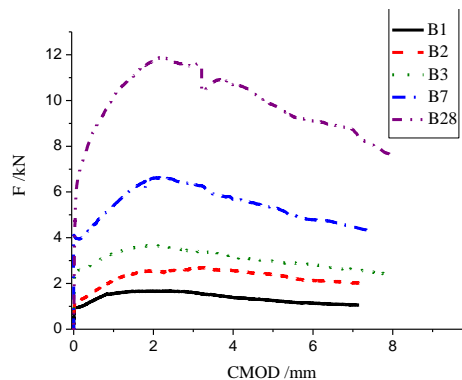


Fig. 10 Typical LOAD Vs. CMOD curves for SFRC composite notched cubes with different curing age

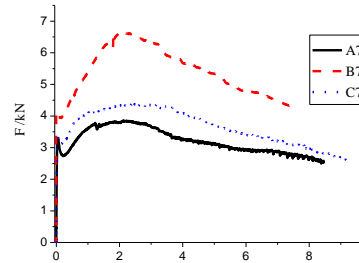


Fig. 11 Typical LOAD Vs. CMOD curves for SFRC composite notched cubes with different fiber ratios(7-day)

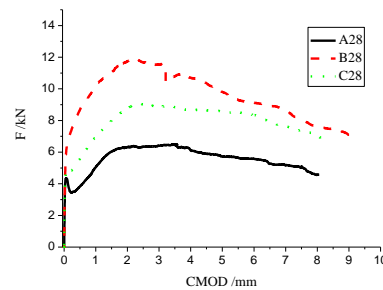


Fig. 12 Typical LOAD Vs. CMOD curves for SFRC composite notched cubes with different fiber ratios (28-day)

drop after the first peak is fading with the increase of curing age. The Dramix steel fiber used in the test has high slenderness ratio and tension strength, thus, even if the CMOD is 6 mm, there also has a higher load value. So, the SFRC specimens have higher fracture energy than the plain concrete specimens.

The typical LOAD Vs. CMOD curves for SFRC composite notched beam with different fiberratios at the age of 7d and 28d are given in Figs. 11 and 12, respectively. The ultimate load increased if mixed suitable steel fiber, though the ultimate load decreased when the fiber content was up to 1.8%, the softening segment was also plump. After the second peak load, the long cured specimens had high strength, but the softening branch of the LOAD Vs. CMOD curves has a faster decline. Though the post-crack load of specimens with fiber content 1.8% is great than the ones with the fiber content 0.6%, and have good fracture toughness, the high mixing is not very economical.

## 5. Numerical simulation

### 5.1 Finite element model

Experimental investigations have highlighted that concrete materials in mode I fracture exhibit a brittle/softening behavior. The SFRC materials show a more ductile behavior compared to those of plain concrete (PC) materials. Fibers bridge cracks on the fracture surface during loading and transfer the load, delaying the coalescence of cracks and the element does not break.

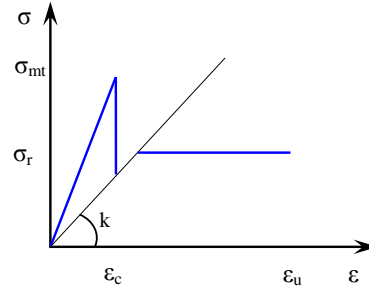


Fig. 13 Tensile behavior of SFRC

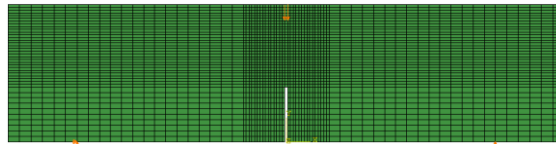


Fig. 14 FEM of three-point bending beam

So far, there is not a type of constitutive model can be used to simulate the SFRC materials. In this study, a finite element software ABAQUS is used to analyze the working performance of SFRC beams under the loading. A concrete damage plasticity model is adopted in the simulation. It assumes that the concrete has two kinds of failure mechanism, which are tensile failure and compress failure. The material mechanical property in this model should be defined by the tensile and compress plastic constitutive relation respectively. The compress plastic constitutive relation of SFRC is the same as PC. The tensile plastic constitutive relation of SFRC is proposed by Olivito and Zuccarello (2010), Han *et al.* (2006) and Lim *et al.* (1987), which is suitable for the SFRC mixed with higher slenderness ratios steel fibers. The tensile plastic constitutive relation of PC is a bilinear tension softening model (Jin *et al.* 2007). In the case of concrete reinforced by steel fibers, the overall behavior is characterized by the brittle behavior of the matrix and by the bonding properties between fibers and matrix. This model establishes a trilinear constitutive behavior model, which is shown in Fig. 13. The model has three segments: (1) Initial linear elastic phase. It is characterized by an elastic modulus and the peak strength of the concrete  $\sigma_{mt}$ ; (2) Crack developing phase. It is characterized by a strain field greater than the limit strain  $\varepsilon_c$  of the matrix; (3) Failure phase. It is characterized by failure phenomena of the overall composite. Indeed, the value of the stress  $\sigma_r$  at damaged conditions represents the ultimate value of stress for strains greater than  $\varepsilon_c$ .

Herein, the failure process of a SFRC beam ( $SF_b$ ) and a plain concrete beam at the age of 7d are simulated. CPS4R (plane stress 4—node simplified integral element) in ABAQUS element family is adopted in this simulation, the sum of the elements and nodes are 2480 and 2604 respectively. A modified Riks iterative method is applied to model the softening curve. Fine meshing is adopted within the crack band. The supports and the loading bar are simulated by analytical rigid bodies. The detailed meshing partitions are shown in Fig. 14.

## 5.2 Numerical analysis

Taking three-point bending of SFRC beam of 7d for example, its cracking deformation and stress distribution in the whole failure process are shown as follows:

It can be seen from Figs. 15 ~ 17 that the opening displacement linearly increases with the increasing load, the maximum tension stress is developed with the crack tip upwards into the concrete along the notch. Because of the existence of the bridged steel fibers, the tension stress will not rapidly decrease to zero, and it would get to a second peak due to the plastic performance of SFRC. Beside the notch surfaces, it will always be a high stress concentration zone. From Fig. 17 (b), it can be seen that, the beam can still support a large stress and the steel fibers bridged between the crack surfaces in the test beam, even though at the ultimate cracking deformations (See Fig. 17(a)).

In order to analyze the influence of steel fibers on fracture properties of SFRC, the stress cloud and a damaged test PC beam are shown in Fig. 18. Once a crack appears, the LOAD-CMOD curve

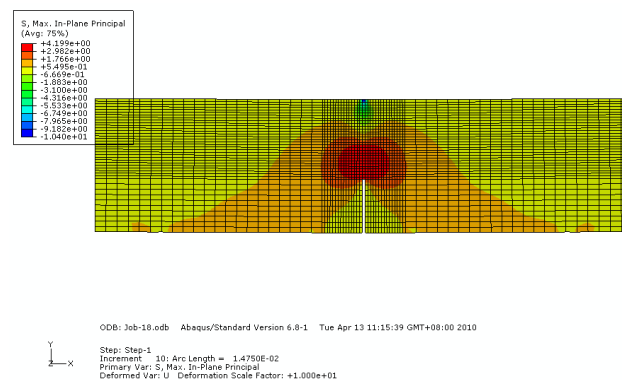


Fig. 15 Initial cracking deformations and distribution of the maximum principle stress (SFRC, 7-day)

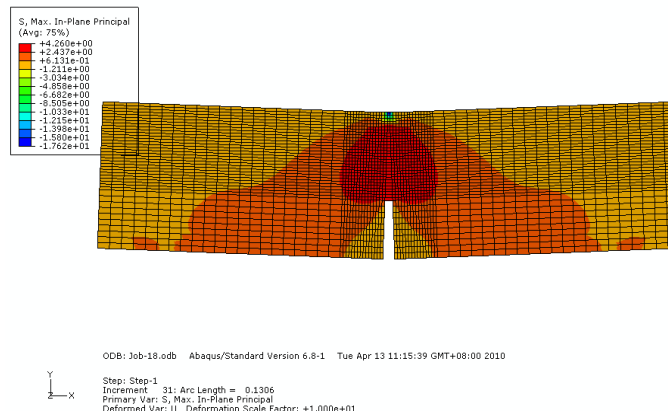
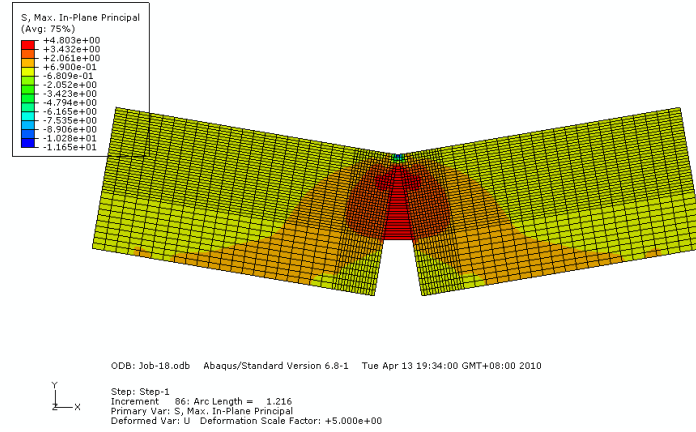


Fig. 16 Cracking deformations and distribution of the maximum principle stress under ultimate load (SFRC, 28-day)

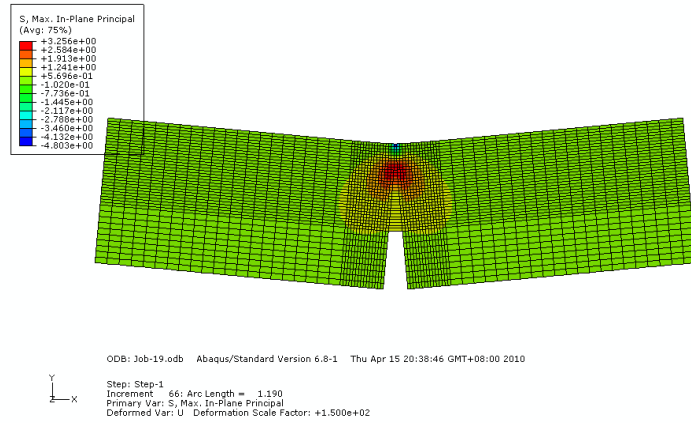


(a) Ultimate cracking deformations and distribution of the maximum principle stress



(b) Post-test aspect of the notched SFRC specimen

Fig. 17 Ultimate cracking deformations and distribution of the maximum principle stress and the corresponding post-test specimen (SFRC, 7-day)



(a) Ultimate cracking deformations and distribution of the maximum principle stress (PC)

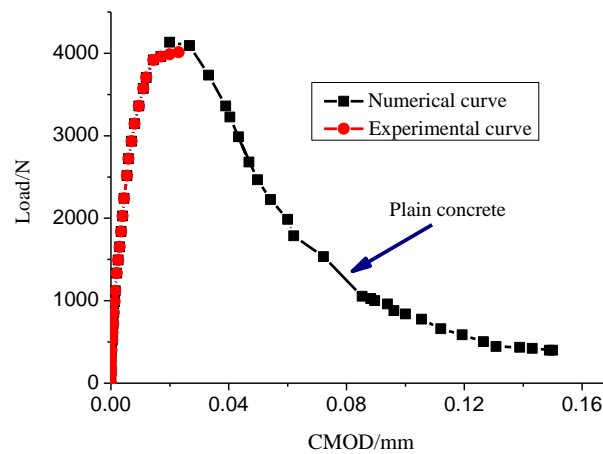


(b) Post-test aspect of the specimens without fibers

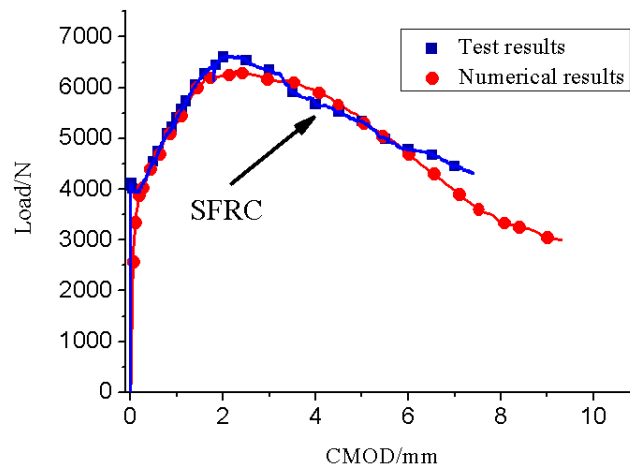
Fig. 18 Ultimate cracking deformations and distribution of the maximum principle stress and the corresponding post-test specimen (PC)

of the specimen will get to the softening segment, and the load will decrease rapidly. Residual tension stress will concentrate in the crack tip transition zone.

Taking out element information above the notch, both the LOAD-CMOD curves and test curves of SFRC and PC at the age of 7 days are shown in Fig. 19. The ultimate load of PC is almost equal to the cracking load of SFRC beam. The numerical results agree well with the test results, the calculation errors are not more than 5%, which indicates that the tension constitutive relation of SFRC and PC are effective when compound with the numerical results, to have a nonlinear calculation. By comparing the Figs. 19(a) and (b), the advantage of SFRC in improving the fracture behavior of PC is obvious.



(a) Test results and numerical results with PC



(b) Test results and numerical results with SFRC

Fig. 19 Comparisons of the simulated LOAD Vs. CMOD curves and the test results (7-day)

## 6. Conclusions

In this paper, the experimental and numerical analysis was carried out in order to investigate the fracture characteristic of SFRC with respect to curing age and different fiber content. The following conclusions can be drawn from this study:

- The cracking load and ultimate load increased with the curing age, and the increasing of fiber content within reasonable limits. If the fiberratios exceed the reasonable value, the enhancement of fracture property with SFRC tends to decrease.

- The two key parameters of fracture toughness and fracture energy are influenced by the curing age and fiber ratios. As curing age increases, matrix strength increases. Additionally, the enhanced bond strength in fiber-matrix interface improved the fracture behavior of SFRC. However, too much increase of fiberscontent in concrete will cause multiple defects of SFRC.

- The test results doindicate that there are internal relationships between fracture toughness and tension strength in the analysis of concrete fracture behavior.Hence, the tension strength can be used to calculate or rectify the fracture toughness values. After all, the splitting strength test is easier than the three-bending test.

- By comparing the LOAD Vs. CMOD curves, it can be seen that the second peak load appeared in all the test specimens. The longer the curing age is, the greater the advantage of Dramix steel fiberis obvious. For the C30 concrete, no fiberfailed under tension. Hence, the high tension strength steel fibers should be used in high strength concrete matrix with a reasonable fiber ratio, and thus it is economical as well.

- In simulating the fracture process test with SFRC and PC, the tensile plastic constitutive relations were introduced, compounding with the finite element software, fracture mechanism analysis can be carried out on SFRC or PC beams effectively. The numerical results are agreed well with the test results.

Furthermore, in future research in the area of high-strength SFRC fracture property shouldbe performed. The outcomes of this research can be very useful in predicting the fracture property trend with the development of concrete strength and steel fiber dosage and selecting reasonable numerical calculation method.

## Acknowledgements

The study of this paper is financially supported by the National Natural Science Foundation of China (Grant Nos.511784013 and 51308503)andthe Major International (Regional) Joint Research Program of China (Grant No. 51320105013), which are thankfully acknowledged. The support by the Alexander von Humboldt (AvH) Foundation of Germany and Sarhad University of Science and Information Technology Peshawar Pakistan are also gratefully acknowledged.

## References

- Aggelis, D.G., Soulioti, D.V., Sapouridis, N., Barkoula, N.M., Paipetis, A.S. and Matikas, T.E. (2011), "Acoustic emission characterization of the fracture process in fiberreinforced concrete", *Constr. Build Mater.*, **25**,4126-4131.
- Bencardino, F., Rizzuti, L., Spadea, G. and Swamy, R.N. (2010), "Experimental evaluation of fiber

- reinforced concrete fracture properties”, *Compos. Part B: Eng.*, **41**(1), 17-24.
- Caggiano, A., Cremona, M. and Faella, C. (2012), “Fracture behavior of concrete beams reinforced with mixed long/short steel fibers”, *Constr. Build Mater.*, **37**, 832-840.
- Carpinteri, A. and Brighenti, R. (2010), “Fracture behaviour of plain and fiber-reinforced concrete with different water content under mixed mode loading”, *Mater. Des.*, **31**(4), 2032-2042.
- Juárez, C., Pedro, Valdez, P., Durán, A. and Sobolev, K. (2007), “The diagonal tension behavior of fiber reinforced concrete beams”, *Cement Concrete Compos.*, **29**(5), 402-408.
- Chalioris, C.E. and Karayannis, C.G. (2009), “Effectiveness of the use of steel fibers on the torsional behavior of flanged concrete beams”, *Cement Concrete Compos.*, **31**, 331-341.
- Han, R., Zhao, S.B. and Qu, F.L. (2006), “Experimental study on the tensile performance of steel fiber reinforced concrete”, *China Civil Eng. J.*, **39**(11), 63-67.
- Jin, N.G., Tian, Y. and Jin, X.Y. (2007), “Numerical simulation of fracture and damage behaviour of young concrete”, *Comput. Concr.*, **4**(3), 221-234.
- Köksal, F., Eyyubov, C. and Özcan, D.M. (2002), “Effect of steel fiber volume fraction on mechanical properties of concrete”, In: *5th International congress on advances in civil engineering*, Istanbul, Turkey, 169-179.
- Kurihara, N., Kunieda, M., Kamada, T., Uchidab, Y. and Rokugob, K. (2000), “Tension softening diagrams and evaluation of properties of steel fiber reinforced concrete”, *Eng. Fract. Mech.*, **65**(2-3), 235-245.
- Li, Z., Li, F., Chang, T.Y.P. and Mai, Y.W. (1998), “Uniaxial tensile behavior of concrete reinforced with randomly distributed short fibers”, *ACI Mater. J.*, **95**(5), 564-574.
- Lim, T.Y., Paramasivam, P. and Lee, S.L., (1987), “Analytical model for tensile behavior of steel-fiber concrete”, *ACI Mater. J.*, **84**(8), 286-298.
- Luccioni, B., Ruano, G., Isla, F., Zerbino, R. and Giaccio, G. (2012), “A simple approach to model SFRC”, *Constr. Build Mater.*, **37**, 111-124.
- Michels, J., Christen, R. and Waldmann, D. (2013), “Experimental and numerical investigation on postcracking behavior of steel fiber reinforced concrete”, *Eng. Fract. Mech.*, **98**, 326-349.
- Mohammadi, Y., Singh, S.P. and Kaushik, S.K. (2008), “Properties of steel fibrous concrete containing mixed fibers in fresh and hardened state”, *Constr. Build Mater.*, **22**, 956-965.
- Olivito, R.S. and Zuccarello, F.A. (2010), “An experimental study on the tensile strength of steel fiber reinforced concrete”, *Composites Part B: Eng.*, **41**(3), 246-255.
- Pereira, E.N.B., Barros, J.A.O., and Camões, A. (2008), “Steel fiber-reinforced self-compacting concrete: experimental research and numerical simulation”, *J. Struct. Eng.*, **134**(8), 1310-1321.
- Qian, C.X. and Indubhushan, P. (1999), “Properties of high-strength steel fiber-reinforced concrete beams in bending”, *Cement Concrete Comp.*, **21**(1), 73-81.
- Shah, S.P. (1991), “Do fibers increase the tensile strength of cement-based matrixes”, *ACI Mater. J.*, **88**(6), 595-602.
- Shah, A.A. and Ribakov, Y. (2011a), “Recent trends in steel fiber high strength concrete”, *Mater. Des.*, **32**, 4122-4151.
- Shah, A.A., Alsayed, S.H., Abbas, H., and Al-Salloum, Y.A. (2012), “Predicting residual strength of non-linear ultrasonically evaluated damaged concrete using artificial neural network”, *Constr. Build Mater.*, **29**(1), 42-50.
- Shah, A.A., Ribakov, Y., (2011b), “Estimation of RC slab-column joints effective strength using neural networks”, *Lat. Am. J. Solid Struct.*, **8**(4), 393-411.
- Shah, A.A. and Ribakov, Y. (2010), “Effectiveness of nonlinear ultrasonic and acoustic emission evaluation of concrete with distributed damages”, *Mater. Des.*, **31**(8), 3777-3784.
- Shah, A.A., Ribakov, Y., and Zhang, C.H. (2013), “Efficiency and sensitivity of linear and non-linear ultrasonic techniques to identifying micro and macro scale defects in concrete”, *Mater. Des.*, **50**(6), 905-1016.
- Shah, A.A. and Hirose, S. (2010), “Nonlinear ultrasonic investigation of concrete damaged under uniaxial compression step loading”, *J. Mater. Civil Eng.*, **22**(5), 476-484.
- Soulioti, D., Barkoula, N.M., Paipetis, A., Matikas, T.E., Shiotani, T. and Aggelis, D.G. (2009), “Acoustic

- emission behavior of steel fiber reinforced concrete under bending”, *Constr. Build Mater.*, **23**(12), 3532-3536.
- Teng, T.L., Chu, Y.A., Chang, F.A., Shen, B.C. and Cheng, D.S. (2008), “Development and validation of numerical model of steel fiber reinforced concrete for high-velocity impact”, *Comp. Mater. Sci.*, **42**(1), 90-99.
- Uygunoqlu, T. (2008), “Investigation of microstructure and flexural behavior of steel-fiber reinforced concrete”, *Mater. Struct.*, **41**(8), 1441-1449.
- Wang, Z.L., Wu, J. and Wang, J.G. (2010), “Experimental and numerical analysis on effect of fiber aspect ratio on mechanical properties of SFRC”, *Constr. Build Mater.*, **24**, 559-565.
- Wang, Q.S., Li, X.B., Zhao, G.Y., Shao, P. and Yao, J.R. (2008), “Experiment on mechanical properties of steel fiber reinforced concrete and application in deep underground engineering”, *J. China Univ. Mining. Technol.*, **18**(1), 64-66.
- Yazıcı, Ş., İnan, G. and Tabak, V. (2007), “Effect of aspect ratio and volume fraction of steel fiber on the mechanical properties of SFRC”, *Constr. Build Mater.*, **21**(6), 1250-1253.
- Zhang, J., Stang, H. and Li, V.C. (2001), “Crack bridging model for fiber reinforced concrete under fatigue tension”, *Int. J. Fatigue.*, **23**(8), 655-670.

CC